

PETROPHYSICS OF THE MORROW FORMATION, SOUTHEASTERN NEW MEXICO

GEORGE A. HILLIS

*Bass Enterprises Production Company
First City Bank Tower
201 Main Street
Fort Worth, Texas 76102*

N.M.O.C.D. Case No. 11713
Bass Enterprises Production Co.
EXHIBIT No. 9
February 20, 1997

ABSTRACT

In 1982, Bass Enterprises applied successfully for tight gas designation for the Morrow Formation over an area of approximately 320,000 acres encompassing the Big Eddy and Poker Lake Federal Units in Eddy County, New Mexico. Relating to this application, a petrophysical study was made to determine the pay section in the Morrow and its in situ permeability.

Initially log and core data were quality controlled, porosity logs were calibrated using core data, and Pickett plots were used to determine the formation water resistivity (R_w) and the formation resistivity factor (F). Subsequently, the R_w and F values were used in determining water saturation. The pay section was then identified by determining the porosity and water saturation cut-offs from porosity versus water saturation crossplots and production tests from zones of varying water saturation.

Standard laboratory measured core data analysed at 200 psi provided the porosity-permeability relationships which allowed permeability data to be obtained using the porosity logs. Using additional core data, a relationship was established between this "surface" permeability and a permeability measured at subsurface conditions more analogous to that of the reservoir. This relationship was used to determine the in situ permeability of the pay section.

This discussion covers several critical aspects of reservoir description, and although the data involved pertain to the Morrow Formation, it is stressed that these principles can be applied to other reservoirs. When possible, such aspects should be investigated more frequently, be it in an exploration or a development program.

INTRODUCTION

In order to qualify a reservoir for tight gas designation, the Federal Energy Regulatory Commission requires it to be demonstrated that the average in situ gas permeability throughout the pay section is less than 0.1 millidarcy. Thus two objectives are defined — determination of the pay section and the in situ permeability of it. These aspects form the theme of this discussion.

Although the regional setting is in southeast New Mexico

and involves specifically the Morrow clastic reservoir, the procedures presented here are very applicable to many other reservoirs, and it is the major purpose of this paper to describe these, using the above theme as the format. The procedures to be presented are as follows:

1. Quality control of porosity and resistivity logs.
2. Porosity determination.
3. Examination of the relationship between core porosity measured at surface conditions and subsurface measured porosity (log).
4. Determination of R_w (formation water resistivity) from porosity-resistivity crossplots and water samples, and determination of F (formation resistivity factor), thus allowing determination of water saturation.
5. Determination of water saturation cut-off for net pay from completion tests.
6. Determination of porosity cut-off for net pay from porosity-water saturation crossplots.
7. Determination of the relationship between core porosity and core permeability (surface conditions).
8. Determination of the relationship between core permeability at surface and subsurface conditions.

Procedures 1 through 6 allow for identification of the pay section, while 7 and 8 relate log porosity to surface permeability, and this in turn to in situ permeability.

Core measurements referred to as being made at surface conditions were in fact made at 200 psi, which is the standard laboratory condition. In the text these conditions are commonly termed surface conditions for clear differentiation from measurements made at subsurface conditions, when pressures of 5,500 to 6,000 psi were used.

Prior to discussing these procedures, a brief geological description of the Morrow Formation is presented.

GEOGRAPHICAL AND GEOLOGICAL LOCATION

Figure 1 illustrates the geographical location of the study area. Superimposed on this geographical map are regional recognized geological features, primarily the Pedernal land mass, the Northwestern shelf, the Delaware basin, the Central Basin platform, and the approximate limits of the Morrow Formation (Meyer, 1966).

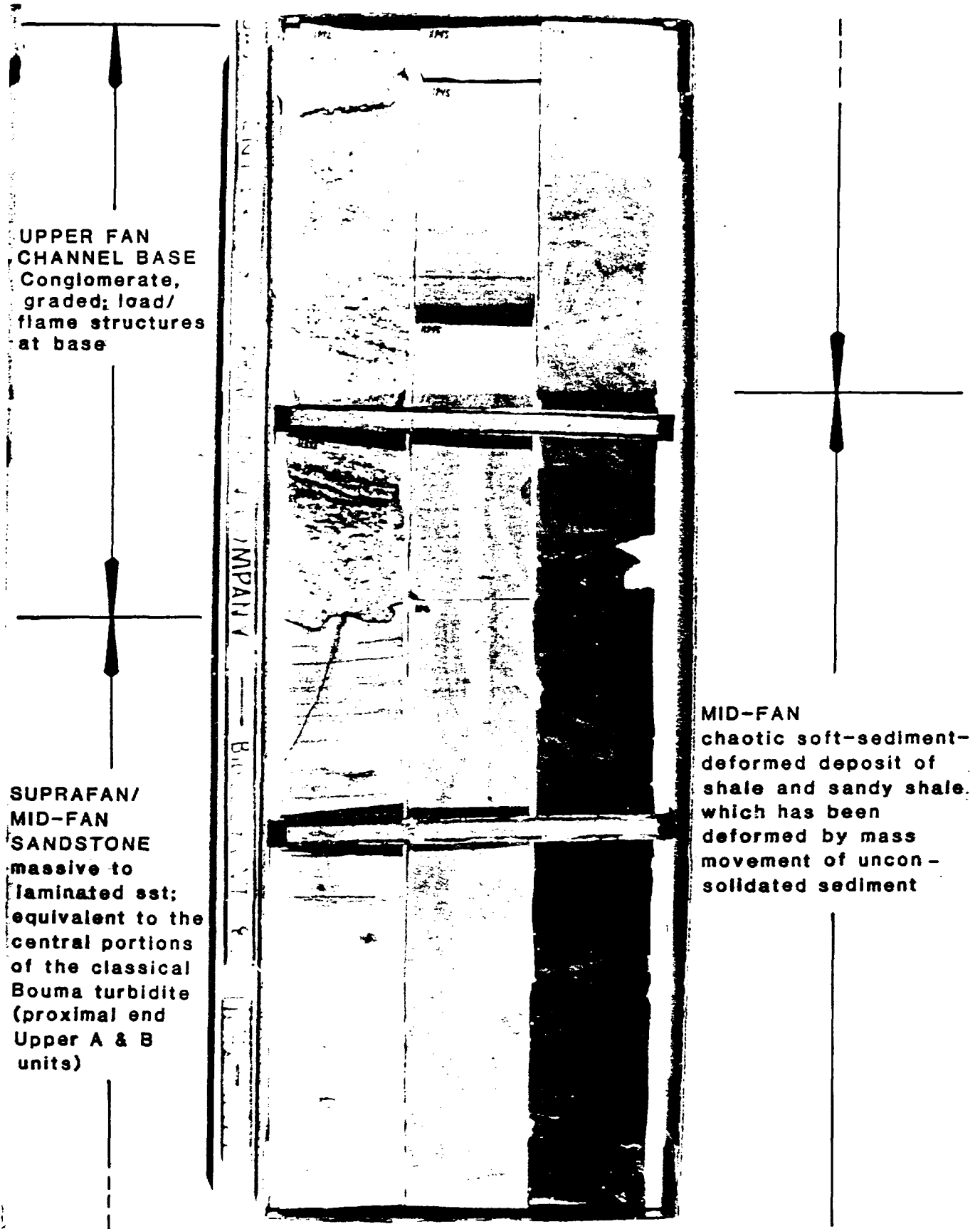


Figure 4. Illustration of features representative of the depositional model

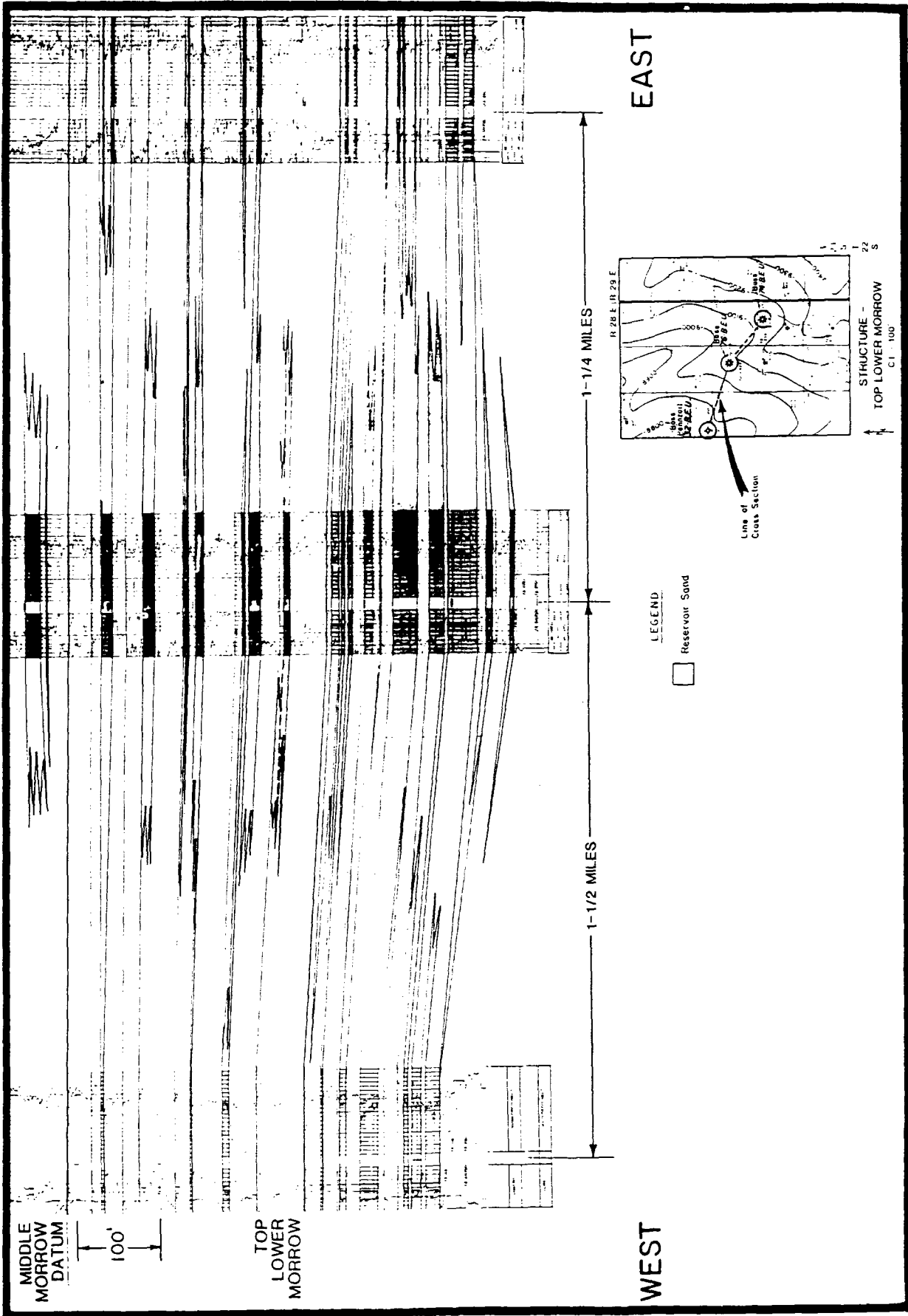


Figure 5. Cross-section illustrating optimum reservoir rock development within paleo-channel.

This is well illustrated by the cross section shown in Figure 5, which cuts across a paleo-channel.

Figure 6 illustrates the present day structure of the top of the Morrow Formation and reflects an average regional dip of 1.3 degrees to the southeast. The average depth to the Morrow taken from the center of the area is 13,600 feet.

CORE CONTROL, MINERALOGICAL ANALYSIS, AND THE ROLE OF CLAYS IN THE RESERVOIR

Figure 7 illustrates the areal location of known Morrow cores in the area. For quantitative work, only cores were used whose (1) gas expansion porosity and grain density were determined using Boyle's Law, and (2) permeability was determined by measuring the flow rate of dry air through the sample which was sealed in a Hassler-type core holder.

For permeability measurements in the Morrow Formation, the latter was important to quality control since, in the 1950s and 1960s, permeability was determined using a Fanchier type holder (for plugs — 2 cm cube) or a Ram type permeameter (for whole core). Both of these are potentially less consistent in accuracy than the modern day rubber sleeve type Hassler holder, primarily due to leakage problems and inability to gauge accurately permeabilities below 0.1 md. Admittedly at that time there was little need to gauge values below 0.1 md.

Based on the above quality control, approximately 50 percent of the cored wells were not used in the quantitative studies. Fortunately, the remaining 50 percent still provide a suitable geographical distribution. All cored wells provide lithological data.

Mineral percentages were obtained on 33 core samples by X-ray diffraction analysis and on nine samples by thin section point counting. From this it is found that the Morrow sands, on average, consist of 86 percent quartz (both as grains and cement), seven percent clays (kaolinite, chlorite, and illite), and three percent calcite, with the remaining four percent made up by chert, siderite, muscovite, pyrite, and heavy minerals. Where intergranular porosity is preserved, the clays are of prime concern during completion and production. Kaolinite (Figure 8, A and B) is of concern since it is chemically stable (and thus not easily chemically removed), is loosely attached to host grains, and has a stacked platelet morphology which is easily broken up causing a "migration of fines" problem (Muecke, 1979; Almon and Davies, 1978). Polymer type clay stabilizers may aid in preventing this movement of fines if used during both drilling and completion operations (Corley et al., 1984). Chlorite (Figure 9, A and B) is also of concern, for although it commonly coats the quartz grains, thereby preserving porosity and permeability by inhibiting quartz overgrowths, it dissolves readily in hydrochloric acid, and iron released from it may reprecipitate as ferric hydroxide which can block pore throats. This problem may be avoided if iron chelating agents and an oxygen scavenger are added with the acid, and if all the acid is recovered before it is spent (Almon and Davies, 1978).

QUALITY CONTROL OF POROSITY AND RESISTIVITY LOGS

It is of little use to calibrate logs for quantitative reservoir parameters if the original porosity or resistivity curves obtained at the well-site are not correct. Methods identified in this study as being of value in obtaining reliable log data include the following:

1. Normalization checks on porosity and resistivity logs should be made using known responses in the area over stratigraphically equivalent zones of constant character — for example, shales (best if over 50 feet thick and continuous in area), tight limes, and anhydrites. Fortunately, if a normalization problem is not identified at the well-site, it may be corrected in the office.

2. Delta rho, caliper, and tension curves displayed on both the 2-inch and 5-inch scales will allow for easier detection of incorrect readings caused by wash-out, tool sticking, or mud build-up on the borehole wall.

3. Repeated log runs over major shows should be made — how often do you pick up a log on a well whose major pay is a 10 to 15 foot sand 300 feet above TD and the repeat is over only the lower 250 feet? If one to two million dollars have been spent drilling to see that sand, it would seem appropriate to run at least one repeat across it.

If a particular good show occurs above the primary one, it should be logged on the way into the hole. If zone of interest is logged twice and the repeat quality is poor, it is wise to run across it one more time.

4. Poor log quality due to tool sticking over zones of interest should be avoided. In the case of a porosity tool like the Density-Neutron, the first pass will be more subject to sticking, due to mud build-up on the wall of the borehole. This first pass tends to "smooth" the borehole, and the next log run is less subject to sticking. The Dual Laterolog Micro-Spherically Focused log (DLL-MSFL), commonly run in southeastern New Mexico, is very prone to sticking in the Morrow Formation because the tool must be held firmly against the borehole wall to obtain valid readings. Accordingly, if sticking is a major problem on the first two attempts at logging the zone(s) of interest, the MSFL tool should be closed, and the log run with the remaining resistivity devices. The logging company should display the "sensor measure point to tension reference point" table on the log. This table lists the distances between the sensor points on the various logging tools and the tension reference point, and allows one to define the depth intervals which have invalid readings due to tool sticking.

POROSITY DETERMINATION

In southeastern New Mexico, the Density-Neutron log is typically displayed using apparent limestone porosity units and thus is compatible with published crossplot charts (Schlumberger, 1977). The one unknown needed to correctly compute the true porosity on a crossplot chart is the matrix density of the rock. The average Morrow reservoir grain density is 2.67 grams per cubic centimeter, based on

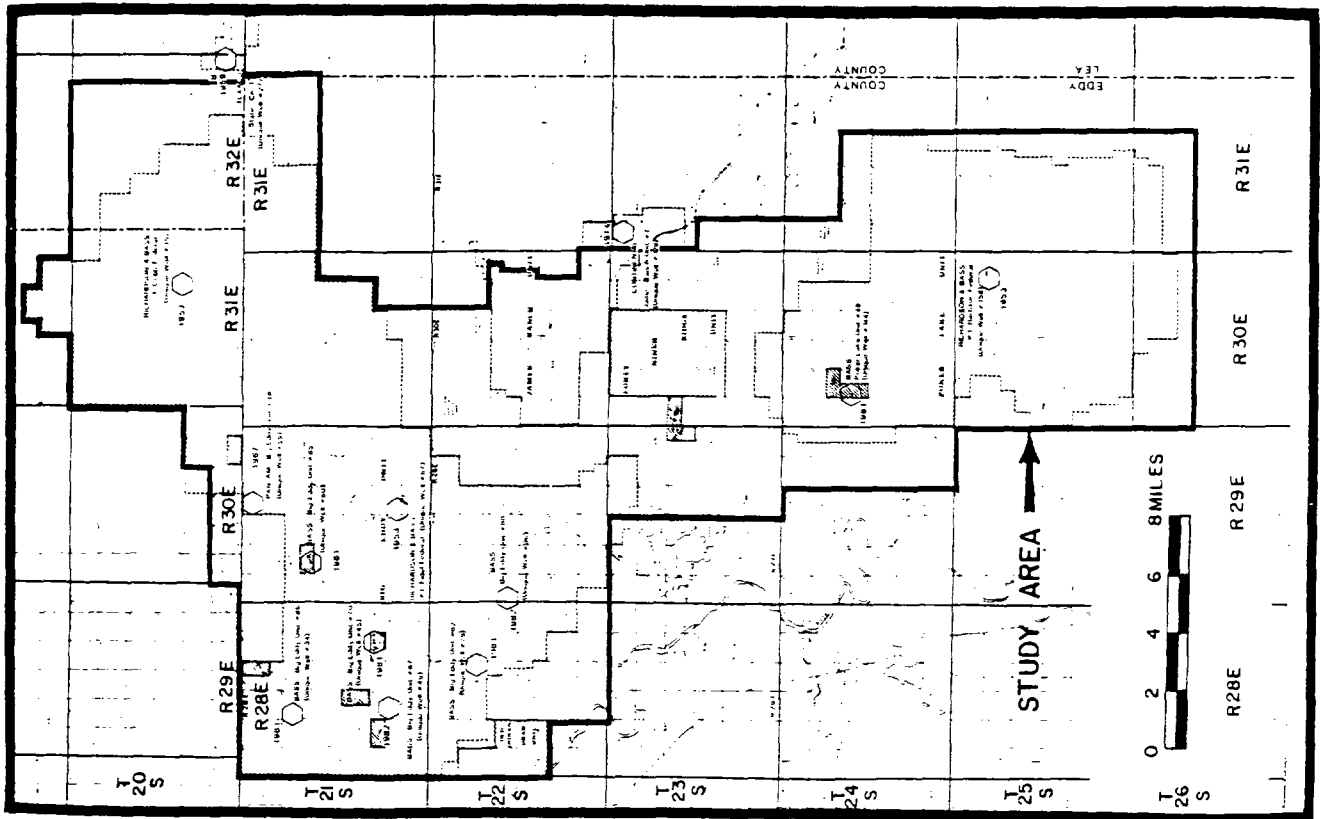


Figure 7. Location of Morrow cores.

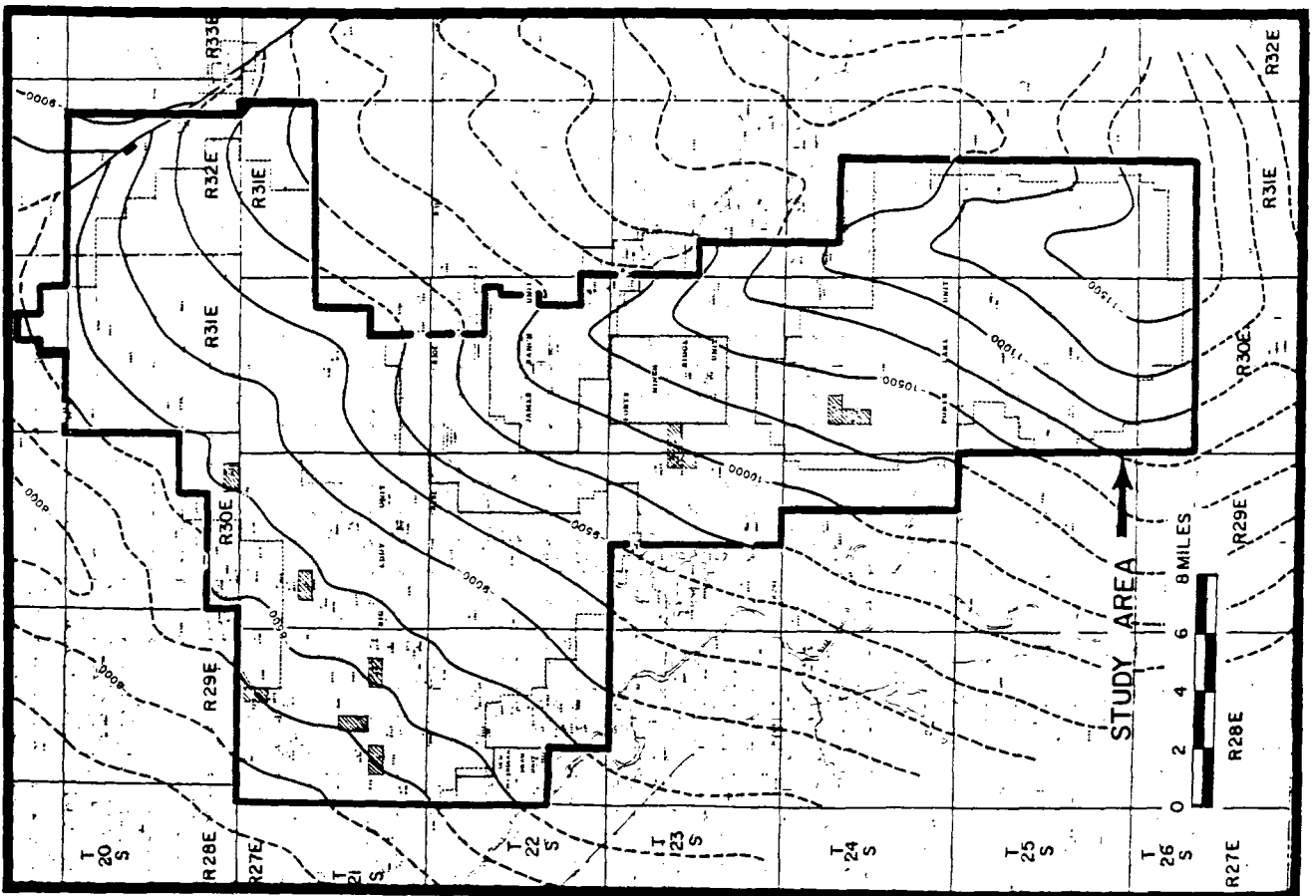


Figure 6. Structure Map - Top of Morrow Formation (contour interval = 250').



Figure 8A SEM photomicrograph illustrating how kaolinite (K) can fill pore space (magnification = 51X, depth = 12,458 ft).



Figure 8B SEM photomicrograph illustrating the platelet morphology characteristic of kaolinite clay (magnification = 450X, depth = 11,760 ft).



Figure 9A SEM photomicrograph illustrating chlorite (C) coating a quartz grain (thus inhibiting quartz overgrowth). Right image is an enlargement of section marked C on left image (magnification: left 200X, right 2000X, depth = 12,464 ft).



Figure 9B SEM photomicrograph illustrating the rosette characteristic of chlorite clay - kaolinite platelets are also present (magnification: 2000X, depth = 12,458 ft).

core data (Figure 10). This matrix density line is displayed on the industry crossplot chart illustrated in Figure 11. Using this chart, the true porosity was computed as follows:

(1) If the crossplot point plots on or below the 2.67 grams per cubic centimeter line, true porosity is read at that point.

(2) If the crossplot point plots above the 2.67 grams per cubic centimeter line, the point is taken to the 2.67 grams per cubic centimeter line, using the illustrated gas correction trend, and the true porosity is read at that point.

It should be noted that Figure 11 is for salt water, liquid-filled holes (fluid density of 1.1 grams per cubic centimeter). This is the common drilling fluid in the area. If wells were drilled with fresh water (fluid density of 1.0 grams per cubic centimeter) the appropriate crossplot chart was used.

Porosity from the Borehole Compensated Sonic/Acoustic log was determined by two methods.

1. A lithology whose grain density is 2.65 grams per cubic centimeter has a matrix velocity (ΔT_{MA}) of 55.6 mic-

roseconds per foot (V_{MA} = 18,000 feet per second), and one whose grain density is 2.71 grams per cubic centimeter has a ΔT_{MA} of 47.6 microseconds per foot (V_{MA} = 21,000 feet per second). By interpolation between these two lithologies, the Morrow reservoir facies, with an average grain density of 2.67 grams per cubic centimeter, has a ΔT_{MA} of 52.6 microseconds per foot (V_{MA} = 19,000 feet per second). This interpolation and related data are illustrated in Figure 12, where also the V_{MA} of 19,000 feet per second relating ΔT to porosity in the Morrow is illustrated on the applicable industry log interpretation chart.

2. Core porosity was plotted against ΔT response for the only cored well with a sonic log in the study area. Figure 13 illustrates this crossplot and also shows the V_{MA} of 19,000 feet per second line obtained by the previous method, thus substantiating the use of this line relating ΔT response to porosity in the Morrow reservoir facies.

ILLEGIBLE

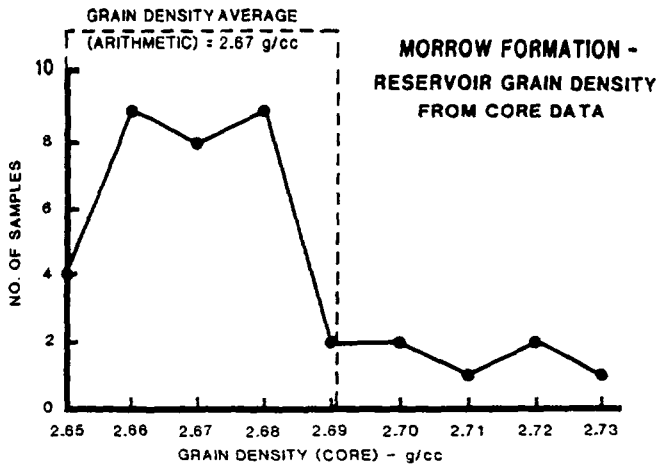


Figure 10. Determination of reservoir grain density from core data.

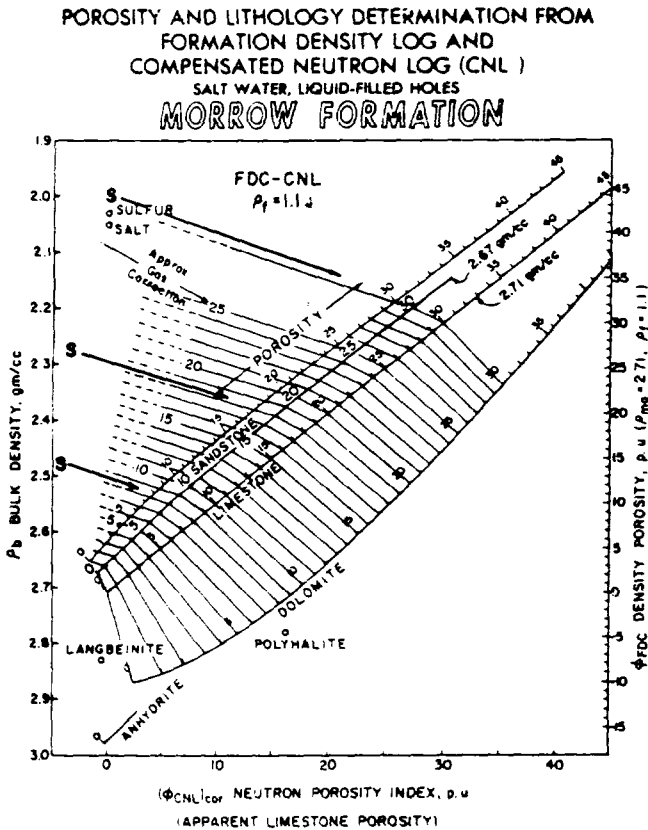


Figure 11. Determination of porosity from Density-Neutron log ("S" indexes gas correction trend recommended by Schlumberger for the Morrow Formation) (with permission of Schlumberger).

RELATIONSHIP OF SURFACE POROSITY (CORE) TO SUBSURFACE POROSITY (LOG)

Figure 14 is a crossplot of core porosity measured at standard laboratory conditions of 200 psi (surface conditions) versus the porosity calculated from the Density-Neutron log by the method previously described. The solid line on the crossplot depicts the line along which the log-derived porosity is equal to the core-derived porosity. Since the porosity calculated from the log represents the porosity at reservoir conditions, this crossplot shows that core-

derived porosity measured at standard laboratory conditions closely matches the porosity at reservoir conditions. In order to confirm this, plug samples were selected and measured by Core Laboratories for porosity at standard laboratory conditions and at a confining pressure of 5,730 psi. Figure 15 illustrates how these two measurements relate to each other. The solid line represents the line along which they would be equal, and the dashed line represents the best-fit line for the crossplotted data. Effectively, there is no significant change in porosity from subsurface to the surface. The confining pressure of 5,730 psi represents the net overburden pressure on a reservoir at a depth of approximately 10,000 feet. Net overburden pressure on a reservoir is the difference between gross overburden pressure, assumed to increase at 1.0 psi per foot, and reservoir fluid pressure. Although the core samples were from approximately 12,000 feet, no significant change had occurred at that stage during the laboratory analysis. For this reason no further pressure was applied to the samples.

DETERMINATION OF R_w FROM POROSITY-RESISTIVITY CROSSPLOTS AND WATER SAMPLES, AND DETERMINATION OF F

Figures 16 and 17 show two methods commonly used to plot porosity versus resistivity in order to define R_w (formation water resistivity) and F (formation resistivity factor). These Φ versus R_t plots are often referred to as "Pickett" plots, or individually as "Log-Log Resistivity-Porosity crossplot" (Log-Log plot) and "Resistivity-Porosity crossplot" (RPC).

In the Log-Log plot (Figure 16), R_t is plotted on a logarithmic scale along the X-axis, and porosity (Φ) on a logarithmic scale along the Y-axis. The S_w = 100 percent line, constructed by drawing a line through the most southwesterly points, intersects the Φ = 100 percent line at an R_t of 0.065 ohmm. This resistivity value is equal to R_w. The slope of the S_w = 100 percent line is equal to the cementation factor (m) and has a value of 2. Assuming the commonly used relationship by Archie that:

$$F = \Phi^m,$$

then

$$F = 1/\Phi^2.$$

In the RPC plot (Figure 17), R_t is plotted on an inverse square root scale along the Y-axis, and porosity is plotted on a linear scale along the X-axis. This graph paper is taken from the Schlumberger 1977 Log Interpretation Chart Book and was designed by Schlumberger for F = 1/Φ². On this plot, the S_w = 100 percent line is constructed by drawing a line through the northwesterly points to the point where R_t equals infinity, and Φ = zero percent. The S_w = 100 percent line is also known as the R₀ line (R₀ is resistivity of formation, with S_w = 100 percent), and its slope is controlled by R_w as follows:

$$\text{Along the } R_0 \text{ line: } R_0 = R_t = \frac{FR_w}{S_w^2}$$

$$S_w = 100 \text{ percent.}$$

$$\text{Thus, } R_0 = FR_w.$$

$$\text{Thus, } R_w = \frac{R_0}{F}$$

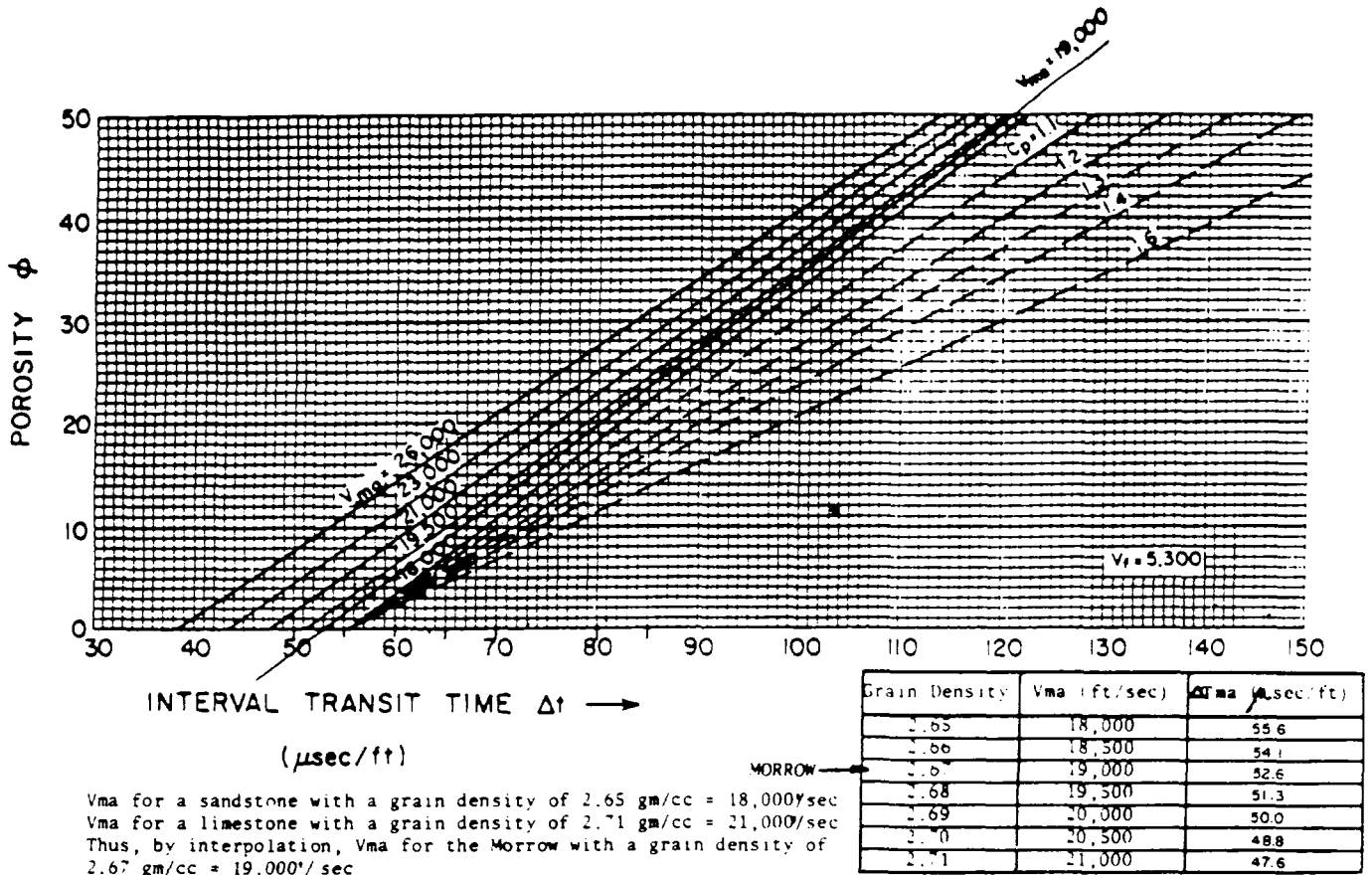


Figure 12. Illustrating matrix velocity for Morrow reservoir, and the interpolation of this velocity knowing the reservoir grain density (with permission of Schlumberger).

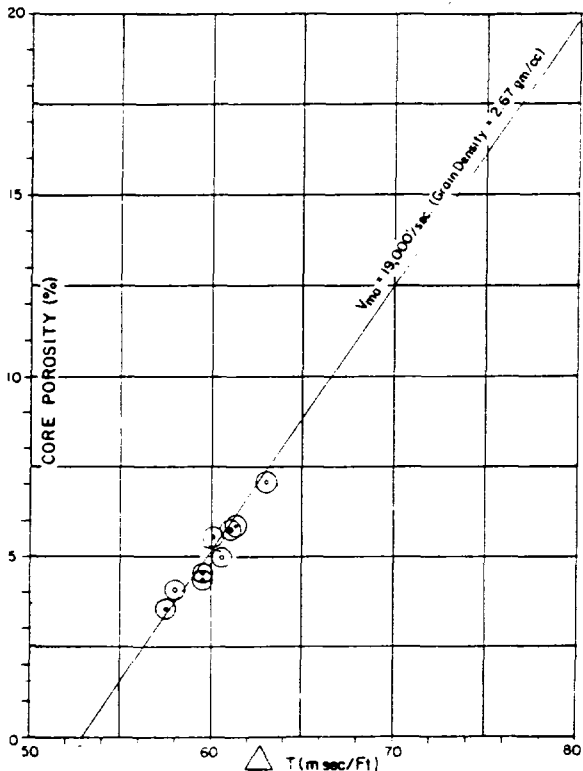


Figure 13. Crossplot of core porosity versus ΔT response, substantiating the earlier interpolated matrix velocity.

For example, at point A, $\Phi = 10$ percent, $F = 100$, and $R_t = 6.5$ ohmm.

$$\text{Thus, } R_w = \frac{6.5}{100} = 0.065 \text{ ohmm}$$

Determination of other S_w lines is as follows:

$$R_t = \frac{FR_w}{S_w^2}$$

For example, $\Phi = 10$ percent, $F = 100$, and $S_w = 0.45$:

$$\text{Thus, } R_t = \frac{100(0.065)}{(0.45)^2} = 32.1 \text{ ohmm}$$

Thus, point B is obtained ($\Phi = 10$ percent, $R_t = 32.1$) and the $S_w = 45$ percent line is obtained by drawing the line from $\Phi = 0$ percent through point B.

Confirmation of an $R_w = 0.065$ ohmm at reservoir conditions using samples of Morrow formation water from 12 wells in the study area is shown on Figure 18.

DETERMINATION OF WATER SATURATION CUT-OFF FOR NET PAY

Production tests of intervals with varying water saturations were examined, and it was found that intervals with water saturations below 45 percent gave water-free or close to water-free completions. Although several completions in zones with 45 percent to 50 percent water saturation also

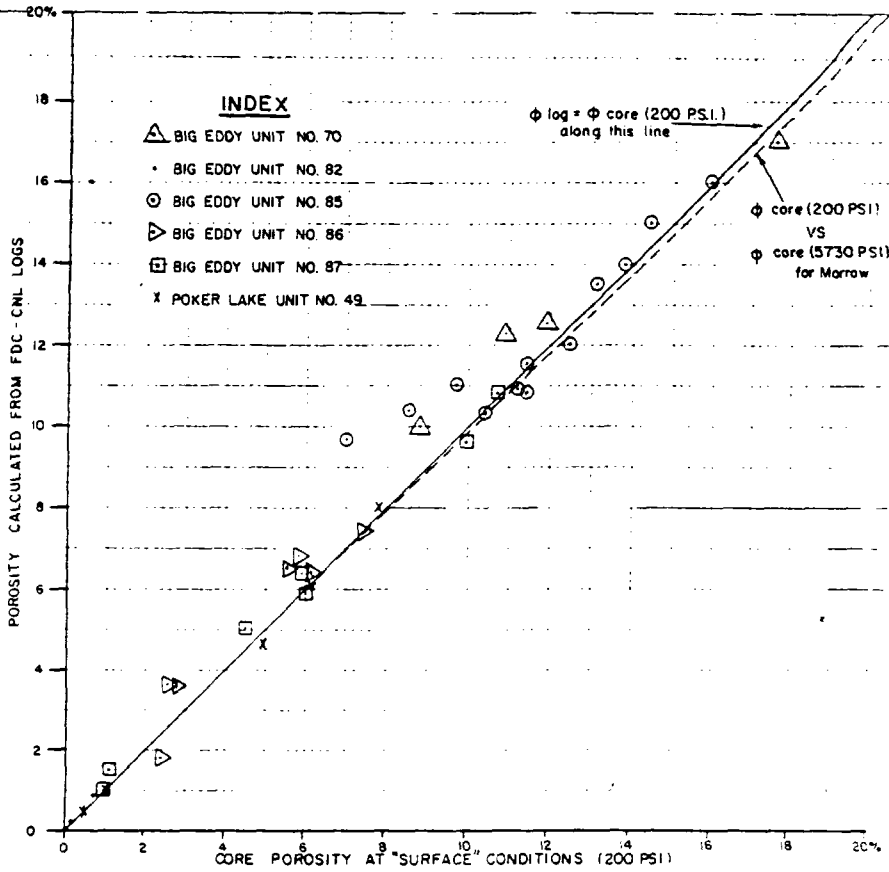


Figure 14. Crossplot of core porosity measured at standard laboratory conditions of 200 psi (surface conditions) versus porosity calculated from the Density-Neutron log.

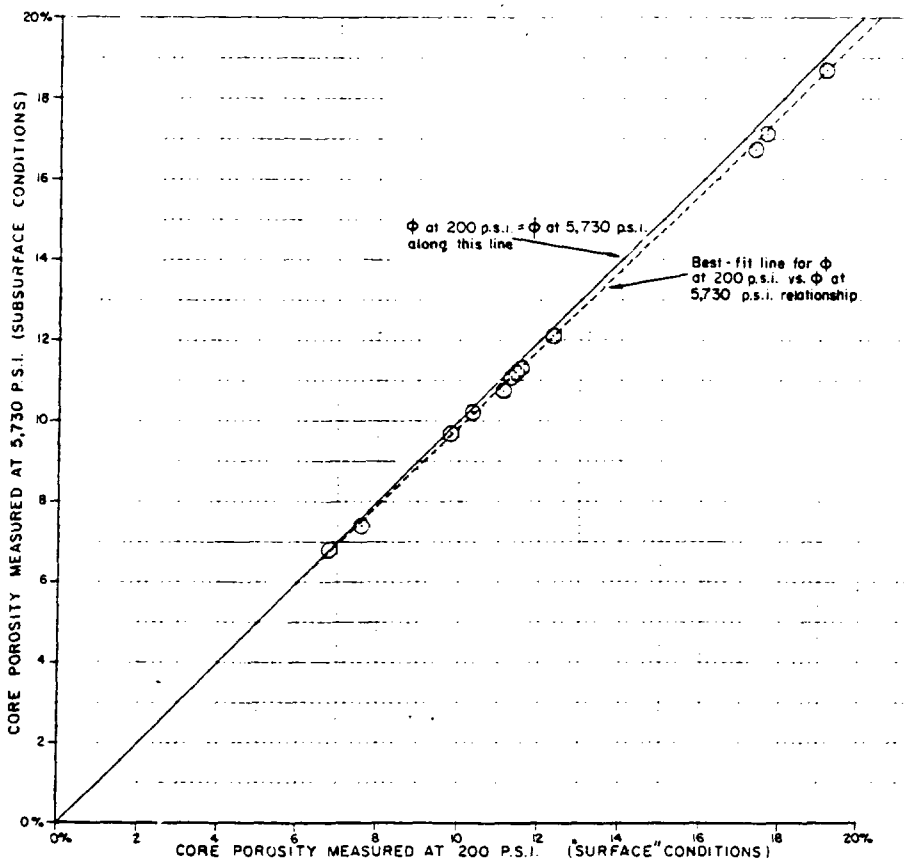


Figure 15. Crossplot of core porosity measured at surface conditions versus core porosity measured at subsurface conditions.

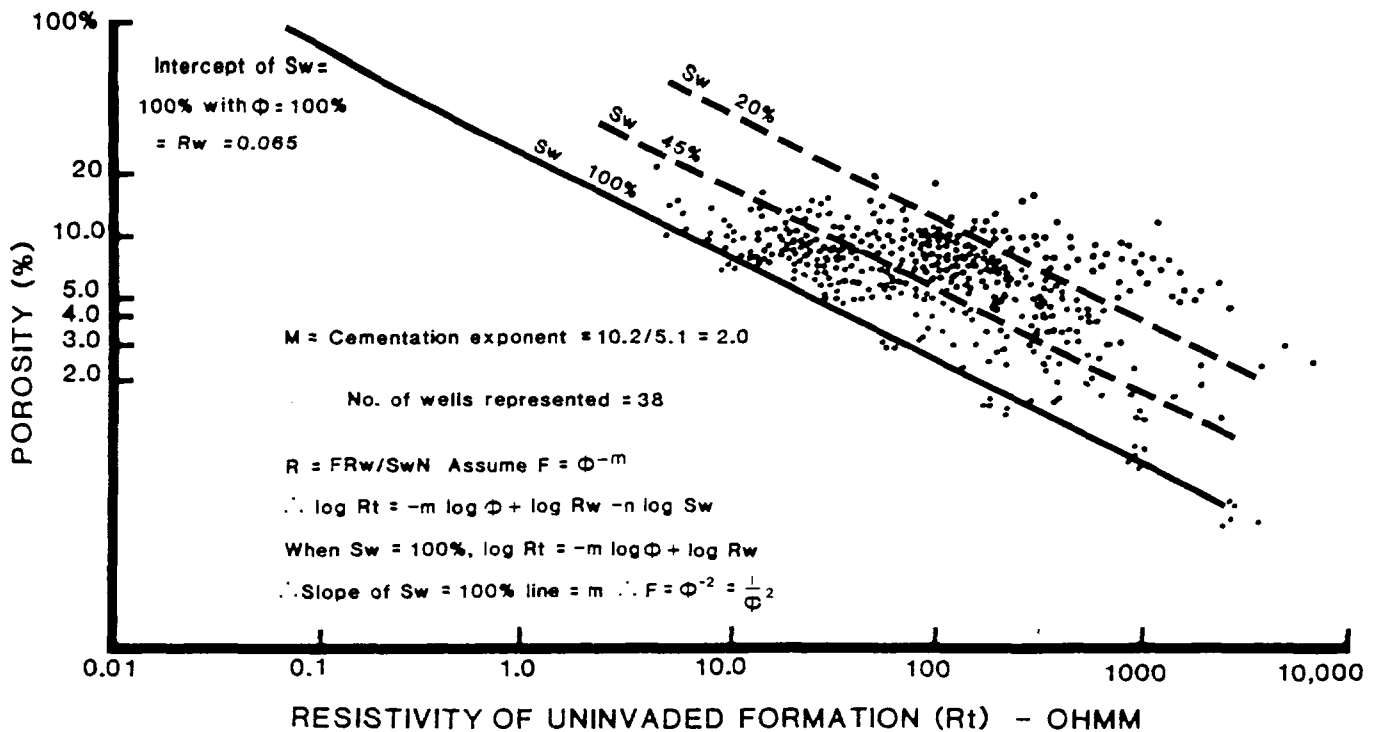


Figure 16. Log-Log Resistivity-Porosity crossplot, illustrating determination of R_w (formation water resistivity) and m (cementation factor).

produced gas, associated water volumes made it uneconomical to produce from these zones. Those with water saturations above 50 percent were water-productive only.

Water saturation (S_w) was calculated by the following equation:

$$S_w = \sqrt{\frac{FR_w}{R_t}}$$

where $F = 1/\Phi^2$, $R_w = 0.065$ ohmm, R_t = resistivity of uninvaded reservoir zone.

DETERMINATION OF POROSITY CUT-OFF FOR NET PAY

Initially in the study, three wells were randomly selected, and individual graphs were made for porosity versus formation water saturation. Zones with porosities above 7 percent were excluded if their water saturations were greater than 50 percent. This eliminated data from zones which were considered to be definite pay on a porosity basis but water productive, due commonly to structural position. The reason for this distinction was to investigate if a porosity versus water saturation plot could serve as an alternative to capillary pressure data in determining the limiting porosity where gas was no longer able to displace interstitial water in the rock.

A common feature identified on these trial wells is a significant decrease in the average S_w going from approximately 2.0 to 3.5 percent porosity (S_w drops from 70 percent to 40 percent), while the average S_w for porosities over 3.5 percent remained relatively constant (25 percent to 30 percent range). Data from 35 additional wells were collected, and a Φ versus S_w plot of these and the three wells above, had similar findings (Figure 19).

It was concluded from this plot that gas was capable of displacing interstitial water in the rock until the porosity was in the 1.5 to 2.5 percent range, and although rock with this porosity was gas bearing, a realistic porosity cut-off for net pay was 3.5 percent. This should not be confused with the current economic porosity cut-off value for the Morrow, 6 to 7 percent.

CORE POROSITY VERSUS CORE PERMEABILITY

Figure 20 is a semi-log presentation of the relationships between porosity and permeability (K) on core samples from six Morrow wells. Core porosity is plotted on an arithmetic scale from 0 to 20 percent porosity and the permeability data are plotted on a logarithmic scale of 0.001 to 1000 millidarcy. It was determined that grain size affected the Φ versus K relationship and that two separate relationships were more accurate. Accordingly, a differentiation has been made on this plot between very fine- to fine-grained and medium- to coarse-grained sands. For example, the permeability in a medium to coarse sand with 10 percent porosity is approximately 12.5 times that in a very fine- to fine-grained sand with 10 percent porosity.

Permeability is probably the single most important reservoir parameter. For instance, knowing that a zone has 10 percent porosity may mean very little unless one is familiar with the Φ versus K relationship for the particular lithology. It is a worthwhile exercise to explore company files for core descriptions and analyses and to make Φ versus K plots for differing lithologies.

Having established that differing Φ versus K relationships (due to grain size) exist in the Morrow sands, the problem is to differentiate very fine- to fine-grained and medium- to

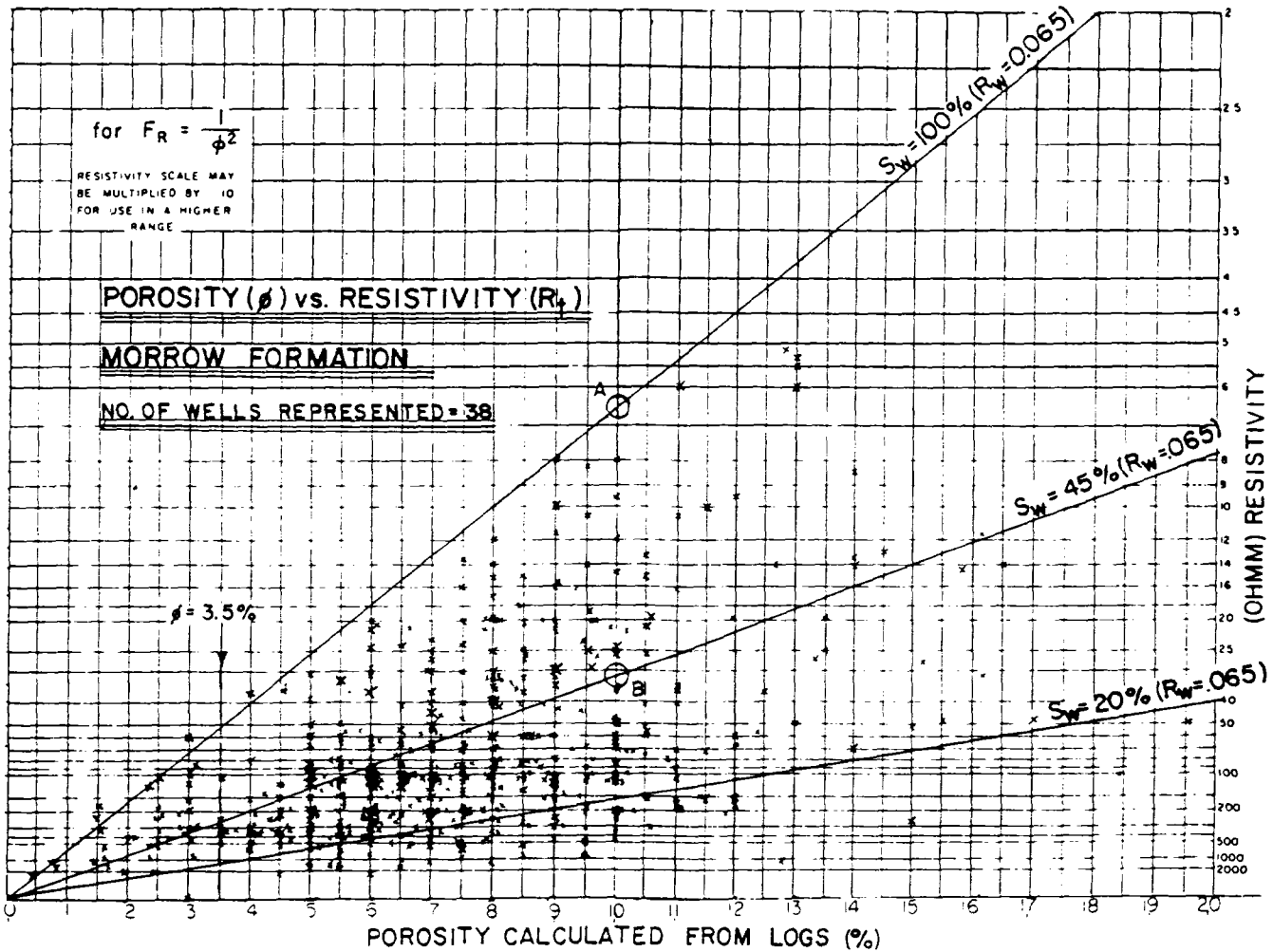


Figure 17. RPC (Resistivity-Porosity crossplot) illustrating determination of R_w .

WELL NAME AND LOCATION	$R_w @ 77^\circ F^{**}$	$R_w @ 200^\circ F^{**}$
BIG EDDY UNIT #35 Sec. 27, T20S-R30E	0.161	0.0652
BIG EDDY UNIT #72 Sec. 3, T21S-R28E	0.1688	0.0676
BIG EDDY UNIT #79-Y Sec. 21, T21S-R28E	0.177	0.0717
BIG EDDY UNIT #78 Sec. 23, T21S-R28E	0.1425	0.0577
BIG EDDY UNIT #66 Sec. 25, T21S-R28E	0.1842	0.0746
BIG EDDY UNIT #39 Sec. 29, T21S-R28E	0.152	0.0616
BIG EDDY UNIT #41 Sec. 35, T21S-R28E	0.1456	0.0590
BIG EDDY UNIT #97 Sec. 35, T21S-R29E	0.148	0.0600
BIG EDDY UNIT #77 Sec. 9, T22S-R28E	0.151	0.0612
BIG EDDY UNIT #68 Sec. 10, T22S-R28E	0.182	0.0737
JAMES "A" #1 Sec. 2, T22S-R30E	0.153	0.0619
GOLDEN LANE FED. #38 #1 Sec. 36, T20S-R29E	0.163	0.0660

R_w AVERAGE (arithmetic) AT $200^\circ F = \frac{0.7802}{12} = 0.0650$

* $77^\circ F$ is temperature at which R_w is commonly measured in Laboratory

** $200^\circ F$ is average reservoir temperature and $R_w @ 200^\circ F$ is obtained from the $R_w @ 77^\circ F$ by the ARPS FORMULA listed below

$$R_{200^\circ F} = R_{77^\circ F} \left(\frac{77 + 6.77}{200 + 6.77} \right)$$

Figure 18. Tabulation of R_w values determined by commercial laboratory water analysis for formation water from 12 wells.

coarse-grained porous sands in a well which has no core. The following factors, illustrated in Figure 21, can be considered in order to make this judgment:

1. Drilling break: the medium- to coarse-grained sands break the best, typically to less than 2 minutes per foot.
2. Samples: while drilling the Morrow section, it is a good idea to change from the more common 10 foot sample interval to a 2 to 4 foot sample interval.
3. Mud cake: the medium- to coarse-grained sands tend to develop a mud cake.
4. Gamma-ray: the medium- to coarse-grained sands tend to have a cleaner, more stable gamma ray.
5. Resistivity: the medium- to coarse-grained sands exhibit resistivity curve separation; the very fine- to fine-grained sands seldom do. This is one of the best indicators, because the resistivity log reflects the permeability of the sand. This author finds himself commonly opening the resistivity log before the porosity log.

0.16 @ 77°

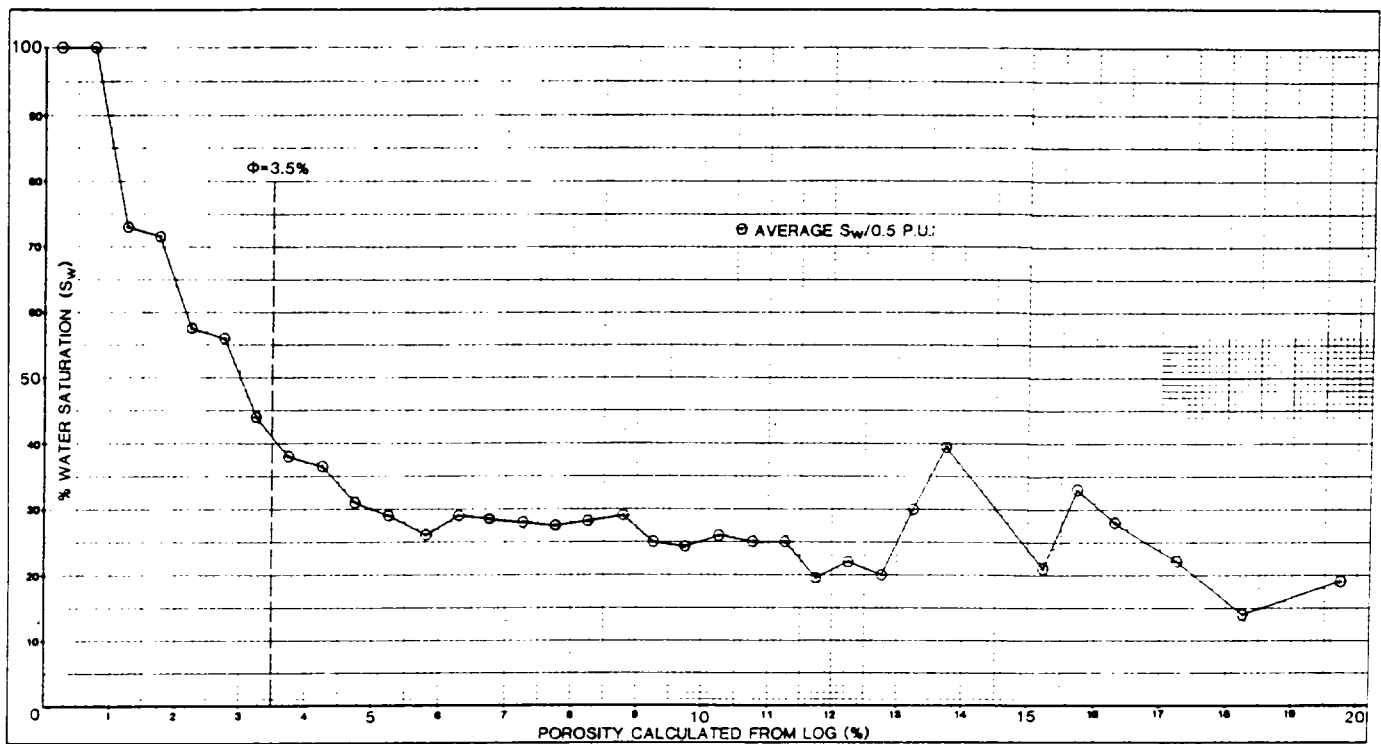


Figure 19. Porosity versus water saturation crossplot (38 wells represented).

**CORE PERMEABILITY
AT STANDARD LABORATORY CONDITIONS
VERSUS CORE PERMEABILITY
AT SUBSURFACE CONDITIONS**

It was shown earlier that porosity measured in a core at standard laboratory conditions of 200 psi (surface conditions) was not significantly different from subsurface porosity. Unfortunately, the same does not hold true for permeability. Plug samples from three wells with a good range of permeabilities were tested by Core Laboratories for their permeabilities at surface and subsurface conditions. Subsurface conditions were achieved in the laboratory by subjecting the plugs to an average confining pressure of approximately 5,700 psi.

Figure 22 is a log-log crossplot of the core permeability (md), measured at subsurface conditions along the X-axis, versus core permeability (md), measured at surface conditions, along the Y-axis. The permeability measured was the permeability to air. The plotted data generate a gently curving, almost linear plot; the two lines are the least squares power-curve-fit lines for the data.

As geologists, we are accustomed to seeing core analyses, and I am sure a lot of us term the permeability presented therein as the permeability of the rock. Consider, then, the data on this crossplot. A surface permeability of 0.1 md is 0.009 md in the subsurface, that is, 9 percent of the surface measured permeability. This increases to 21 percent at 1.0 md (surface), and 77 percent at 100 md (surface).

The confining pressure used represents the net overburden pressure on a reservoir at a depth of approximately 10,000 feet, which is shallower than the average depth to the Morrow in the area, but during testing the major loss of permeability occurred before a pressure of 3,000 psi was

attained. The reduction in permeability above this pressure was very slight and was negligible above 5,000 psi. Several publications (Core Laboratories, 1977; Jones and Owens, 1980; Sampath and Keighin, 1982; Thomas and Ward, 1972) have shown that for rocks in that range of permeability to be affected by overburden pressure, the initial surface permeability is reduced approximately 50 percent by the time the confining pressure has increased 500 to 1,000 psi, and approximately 80 percent at 2,000 to 3,000 psi.

Also illustrated by a dashed line on Figure 22 is a relationship between surface and subsurface permeability previously reported by Jones and Owens (1980). The "Amoco" line is based on data from more than 100 cores of tight gas sands from five formations which vary from 0.02 to 0.55 md. in surface permeability.

SUMMARY

The petrophysical methods described in this paper allowed for definition of the pay in the Morrow Formation and determination of its in situ permeability. The following is an outline of the steps taken.

A. Pay Section Identification

- quality control of log and core data
- porosity (Φ) determination
- determination of the formation water resistivity (R_w) and the formation resistivity factor (F) using Pickett plots.
- determination of water saturation using the above Φ , R_w , and F data.
- determination of the water saturation cut-off for net pay from production tests of zones with varying water saturations.
- determination of the porosity cut-off for net pay using porosity versus water saturation crossplots.

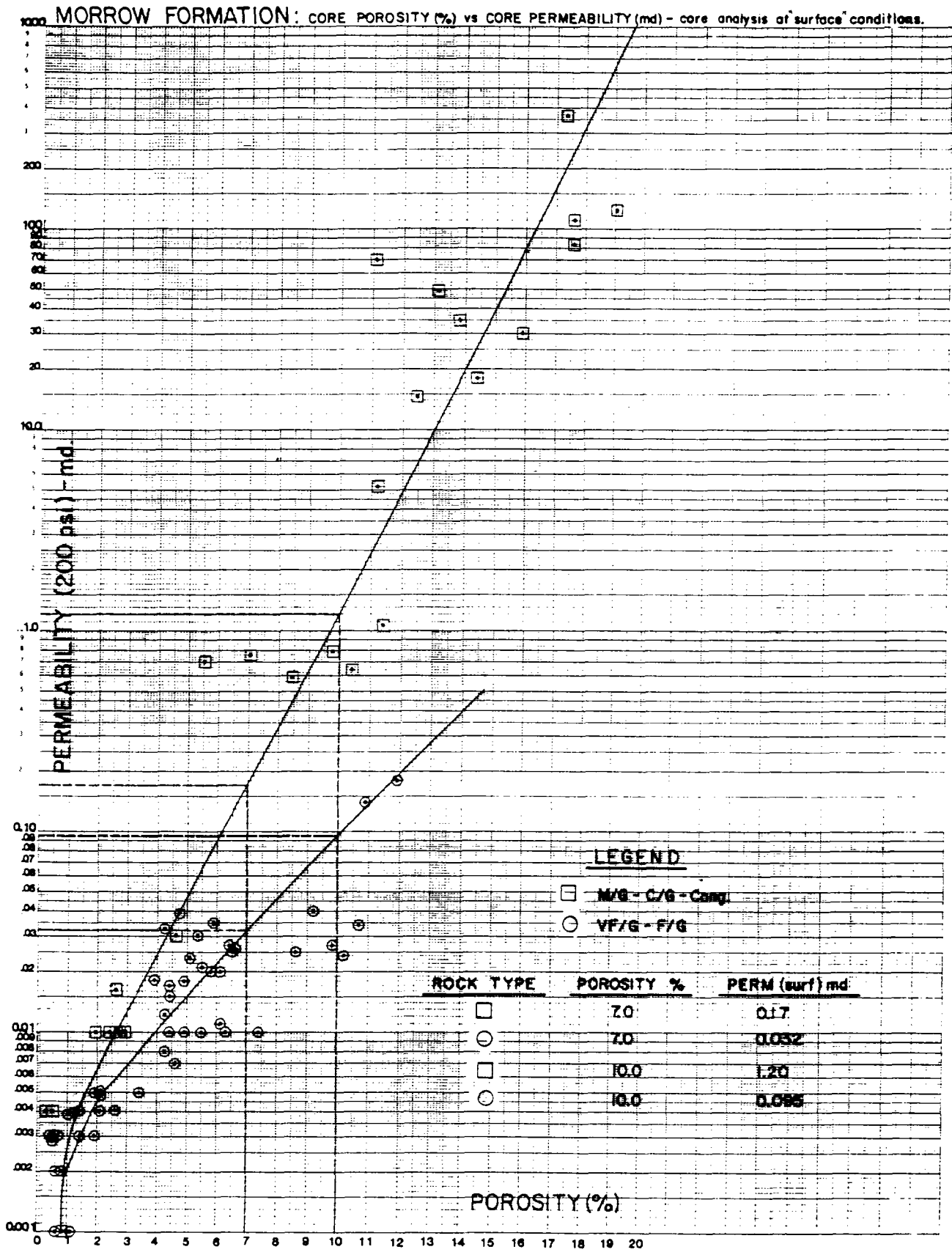


Figure 20. Core porosity versus core permeability. Both parameters measured at standard laboratory conditions of 200 psi (surface conditions) crossplot.

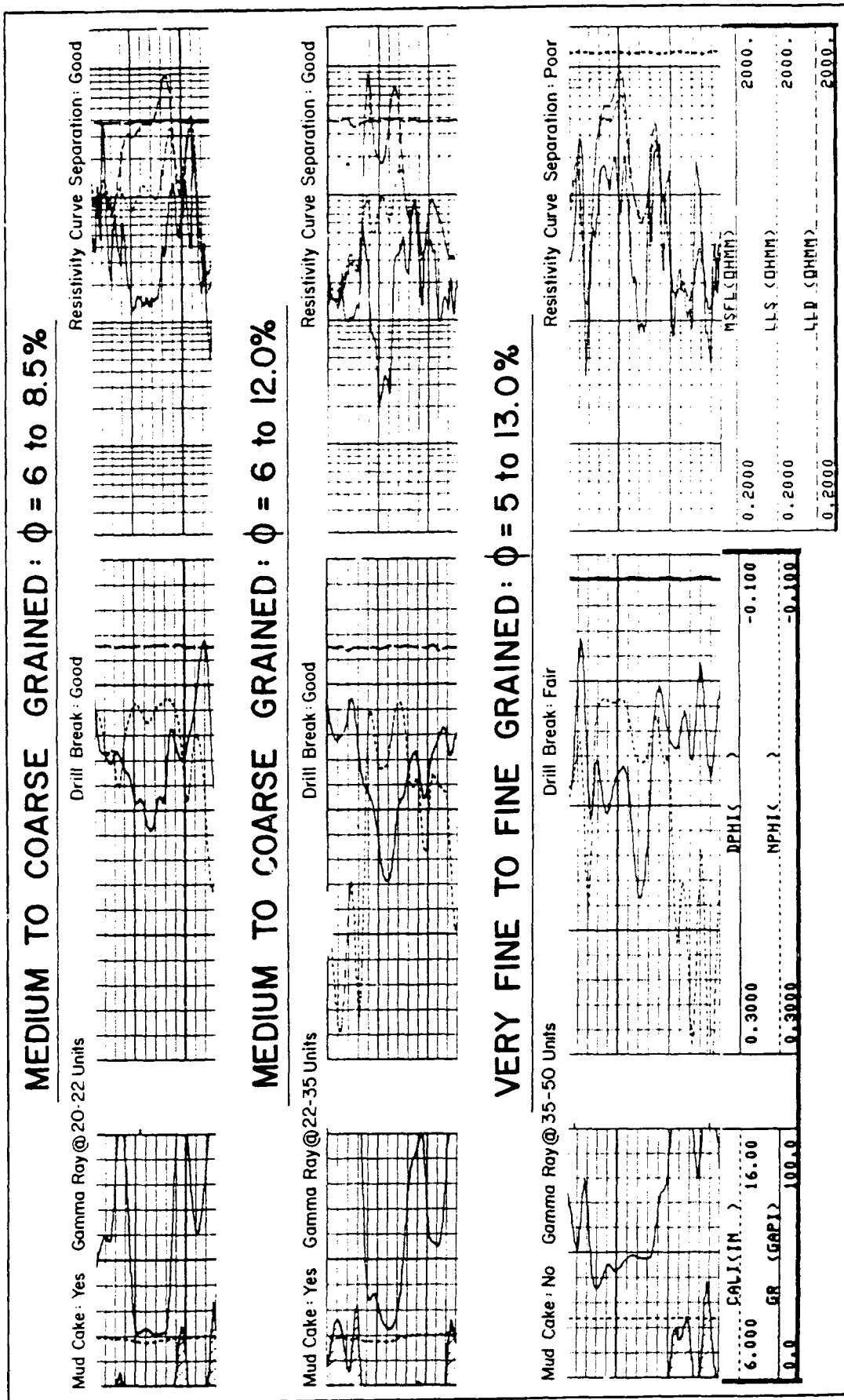


Figure 21. Illustrating log characteristics of medium to coarse grained sands versus those of very fine to fine grained sands.

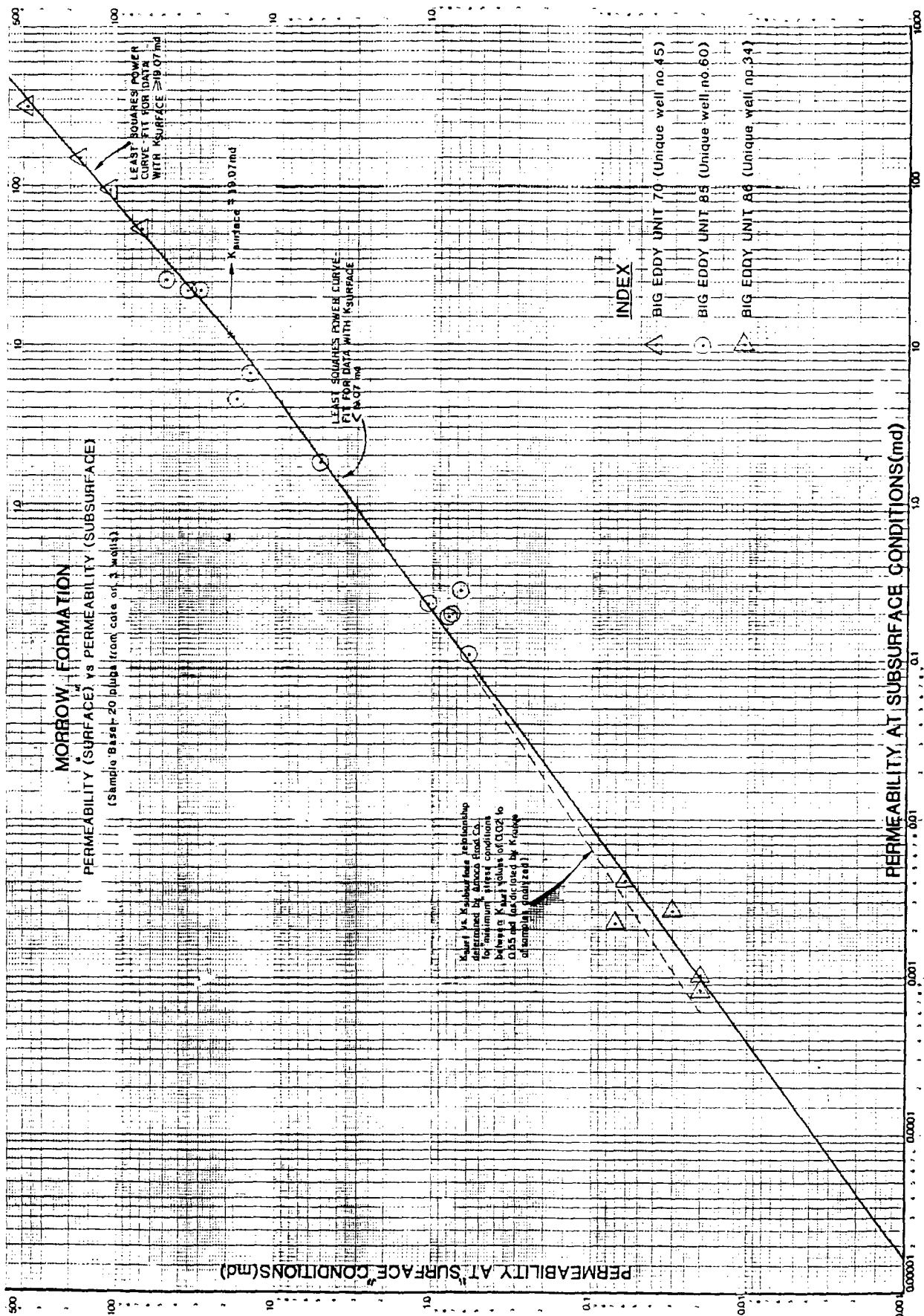


Figure 22 Core permeability at standard laboratory conditions (surface conditions) versus core permeability at subsurface conditions.

B. In Situ Permeability of the Pay Section

- determination of the relationship between core porosity and core permeability measured at standard laboratory conditions ("surface" conditions) and the use of this data in conjunction with the porosity logs to obtain the surface permeability of the pay. Differing porosity-permeability relationships due to grain size variations were established for two groups of sand. Recognition of the different sand groups in a well was based on drilling behavior and log characteristics.
- determination of the relationship between core permeability at surface and subsurface conditions, and the use of this to convert the surface permeability value of the pay to an in situ permeability.

Although the Morrow Formation has been addressed in this discussion, these methods of reservoir description can be applied elsewhere in both exploration and development programs. For this reason, the author has diverged from the

theme to enlarge upon those aspects which need to be considered more often, specifically the quality control of logs, obtaining R_w and F from log data, porosity-permeability relationships for differing rock types, and in situ permeability.

ACKNOWLEDGEMENTS

I wish to thank Bass Enterprises Production Company for giving me the opportunity to do the original study and for supporting me in the preparation and presentation of this paper. Many thanks to Mr. James Greve for guidance in the original work, harassment to write the paper, and reviewing the paper; to Mr. Stewart Henry for his support and review; to Ms. Donna Koesters for her review; to Messrs. Carroll Smith, David Carrizales, and Ms. Lisa Herrera for the illustrations and slide preparation; to Ms. Debbie Curran for typing the manuscript; and to my wife Elizabeth for her support throughout.

REFERENCES

- Almon, W.R., and D.K. Davies, 1978, Clay technology and well stimulation: Gulf Coast Assoc. Geol. Soc., Trans., v. 28, p. 1-6.
- Basan, P.B., 1984, Well completion and stimulation — solutions may add to problems: Drill Bit, April, 1984, p. 23-25.
- Core Laboratories, Inc., 1977, Fundamentals of Core Analysis for West Texas and Southeast New Mexico: 102 p.
- Core Laboratories, Inc., 1977, Special Core Analysis: p. 137-153.
- Corley, W.T., D.L. Dorsey, and T.L. Venus, 1984, Polymer drilling fluid provides nondamaging inhibition: Oil and Gas Jour., July, 1984, p. 52-57.
- Fertl, W.H., and E. Frost, 1980, Evaluation of shaly clastic reservoir rocks: Jour. Petrol. Tech., September, 1980, p. 1641-1646.
- Foster, L., and B. Halepeska, 1974, Improved stimulation fluid for Morrow Sand, southeastern New Mexico: Soc. Petrol. Engin. of AIME, SPE Paper No. 4802.
- Hilchie, D.W., 1982, Advanced Well Log Interpretation: 350 p.
- Hilchie, D.W., 1982, Advanced Openhole Log Interpretation: 330 p.
- Jones, F.O., and W.W. Owens, 1980, A laboratory study of low-permeability gas sands: Jour. Petrol. Tech., Sept., 1980, p. 1631-1640.
- Meyer, R.F., 1966, Geology of Pennsylvanian and Wolfcampian rocks in southeast New Mexico: New Mexico Bur. Mines Mineral Res., Mem. 17, 123 p.
- Muecke, T.W., 1979, Formation fines and factors controlling their movement in porous media: Jour. Petrol. Tech., Feb. 1979, p. 144-150.
- Osaba, J., R. Gist, and H. Carroll, 1981, Log evaluation techniques in Uinta Basin found faulty: World Oil, June, 1981, p. 236-244.
- Sampath, K., and C.W. Keighin, 1982, Evaluation of pore geometry of some low-permeability sandstones — Uinta Basin: Jour. Petrol. Tech., Jan., 1982, p. 65-70.
- Sampath, K., W. Rose, and C.J. Raible, 1981, Special core analysis for western tight sands: U.S. Dept. Energy, May, 1982, Paper DOE/BC 00042-41 (DE82013670).
- Schlumberger, 1974, Volume II — Log Interpretation Applications: 117 p.
- Schlumberger, 1977, Log Interpretation Charts: 83 p.
- Scholle, P.A., and D. Spearing, 1982, Sandstone depositional environments: Amer. Assoc. Petrol. Geol., Mem. 31, 405 p.
- Siemers, C.T., R.W. Tillman, and C.R. Williamson, 1981, Deep-water clastic sediments — a core workshop: Soc. Econ. Paleont. Mineral., Core Workshop No. 2, p. 1-44.
- Simon, D.E., and P. Underwood, 1977, Morrow stimulation in southeast New Mexico: Petrol. Engin. of AIME, SPE Paper No. 6375.
- Thomas, R.D., and D.C. Ward, 1972, Effect of overburden pressure and water saturation on gas permeability of tight sandstone cores: Jour. Petrol. Tech., Feb., 1972, p. 120-124.
- Walker, R.G., 1978, Deep-water sandstone facies and ancient submarine fans: Models for exploration for stratigraphic traps: Amer. Assoc. Petrol. Geol., Bull., v. 62(6), p. 932-966.

CURRENT AND FUTURE TRENDS IN GEOLOGICAL RESEARCH AND APPLICATIONS

E. L. JONES

*Mobil Research and Development Corporation
P.O. Box 81904
Dallas, Texas 75381*

ABSTRACT

It is a high risk venture to predict trends for any science, because new discoveries or new demands can change the directions that are seen at present.

A major geological trend is the participation of geology in reservoir management from time of discovery through the life of a field. A significant task for the geologist in reservoir management is to participate in selecting the appropriate enhanced oil recovery (EOR) method and in its application. As a consequence of these tasks, there is a change in geological applications in production geology from the traditional descriptive aspects to a more quantitative approach.

Exploration management also requires a predictive role for geology. This includes pre-drilling predictions

of reservoir quality and geometry, of aspects of the reservoir fluids including degree of prospect fill-up, and of migration routes.

To refine and expand these predictive capabilities, the combination of geology with the other earth sciences, particularly geophysics and geochemistry, will continue to expand in scope.

Certainly not all of the current and future trends in geology have been identified in this discussion. It seems obvious, however, that these expanded roles for geology should ensure that it will continue to have a significant place in both the exploration and production aspects of the petroleum industry.